Dear Noriaki Horiuchi and Reviewers,

Thank you very much for handling our manuscript. We are sincerely grateful for the reviewers' comments. In the past six months, we have updated the lasing results and written format. We believe the current results well address all the issues raised in the first round of review, especially on the soundness of "phonon pumping". Thanks to reviewers' advice, the quality of our manuscript has been improved significantly in the following aspects:

1. In this revision, we updated Fig. 1a to articulate our new-type *phonon-pumping* mechanism. Our anomalous temperature-dependent lasing threshold with $\partial P_{th}/\partial T<0$ totally differs from previous vibronic lasers with *phonon-assisted* spectral broadening mechanism ($\partial P_{th}/\partial T>0$). We consider this work represents a great breakthrough innovation for laser physics and technology. To make this phonon-pumping work, several conditions have to be satisfied simultaneously: (1) suppression of normal lasing processes, since they usually overwhelm phonon-involved transitions, (2) a moderate electron-phonon coupling intensity, (3) sufficiently large phonon density of states modulated by temperature, (4) selection rules that rely on both electronic and lattice symmetry.

2. Using Nd:YVO_4 crystal as an example, we verified this novel phonon-pumping mechanism in experiments. In previous studies, Nd:YVO_4 was not considered as a vibronic laser crystal owing to its extremely weak electron-phonon coupling effect (S~0.005), and it mainly has four discrete lasing wavelengths at 914, 1064, 1086, and 1342 nm. Our experimental results break this limitation and demonstrate that Nd^{3+}-ion also holds interesting electron-phonon coupling and vibronic lasing behaviors. Its lasing threshold exhibits a negative temperature dependence of $\partial P_{th}/\partial T<0$ in the 295-338 K range. In addition, we give a temperature-dependent rate equation to describe population inversion in the phonon-pumping process.

3. We gave a *power-temperature transition diagram* between phonon-free 1064 nm and phonon-pumped 1176 nm laser. A distinct temperature threshold T_{th} is a manifestation of our phonon-pumping mechanism.

4. We measured the temperature-dependent lasing wavelengths and analyzed the relations between wavelength shift and the electron-phonon coupling effect.

5. We realized a *laser wavelength tuning* for the phonon pumping process. A tunable phonon-pumped laser at 1168 and 1176 nm involving one E_g or A_{1g} mode phonon was realized in Nd:YVO_4 crystal.

6. We also obtained similar phonon-pumped lasers at 1151 and 1166 nm in Nd:YAG crystal, hence indicating the high expansibility of our proposed phonon-pumping mechanism for various solid-state laser materials.

7. We further presented a yellow laser generation at 588 nm by frequency-doubling conversion, representing a potential application for phonon-pumped lasing.

The **conclusive evidence** for our phonon-pumping mechanism is successfully obtained.

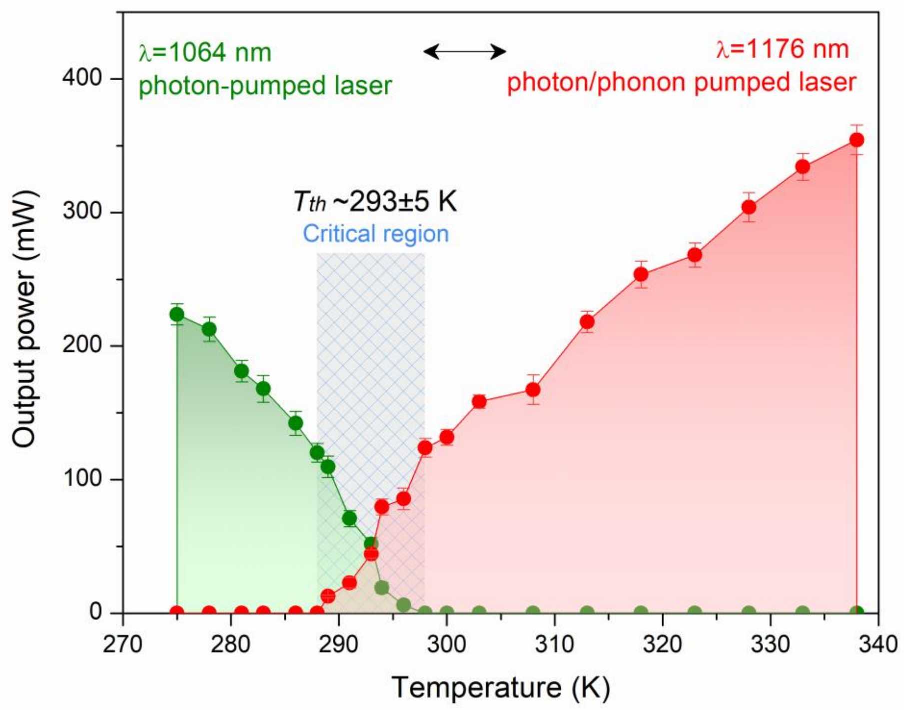

Figure 4a. Power-temperature transition diagram of phonon-free 1064 nm and phonon-pumped 1176 nm laser. The critical region represents the emergence of phonon-pumping process. T_{th} is a temperature threshold for phonon-pumped lasing. The incident power kept unchanged at 7.6 W.

All these new results are added to the revised manuscript and supplementary materials. We believe the current version does meet the strict standards on novelty, innovation and impact for publication in ***Nature Photonics***.

Yours sincerely,

Haohai Yu, Huaijin Zhang and Yan-Feng Chen (On behalf of all authors)

Response to reviewer's comments

Reviewer #1

Comment:

In this work Fu et al. demonstrate phonon assisted photon laser using specific-symmetry phonons. While the work has been performed in great depth and experimental results support the hypothesis of positive phonon contributions, I have certain concerns on the claim of lasing and the written format of the paper. Some of the suggestions and concerns are given below:

1. *Authors should clearly cite appropriate literatures to highlight the knowledge gaps in the introduction and make efforts to underline the past efforts in the area.*

Response:

Thank you for your comments.

In the revision, we cited relative references to identify a long-time problem in the solid-state laser field. A summarized graph was plotted in Fig. R1. In previous reports, to the best of our knowledge, almost all solid-state lasers prefer low temperatures to get lower lasing threshold and higher slope efficiency, including ruby laser, Ti:sapphire, Yb:YAG, Tm:YAG, Ho:YAG, Er:GGAG, Pr:YAP, Fe:ZnSe, Nd:YVO_4 (λ=1064 nm). In Fig. R1, all of them have a positive slope with $\partial P_{th}/\partial T$>0, agreeing with common sense for solid-state vibronic lasers.

However, for our laser, its $\partial P_{th}/\partial T$ is negative, namely high-temperature is favorable for reducing lasing threshold. Such an anomalous behavior can be attributed to a distinctive phonon-pumping mechanism. In addition, our vibronic laser exhibits a relatively high lasing threshold owing to the weak emission intensity of fluorescence satellites.

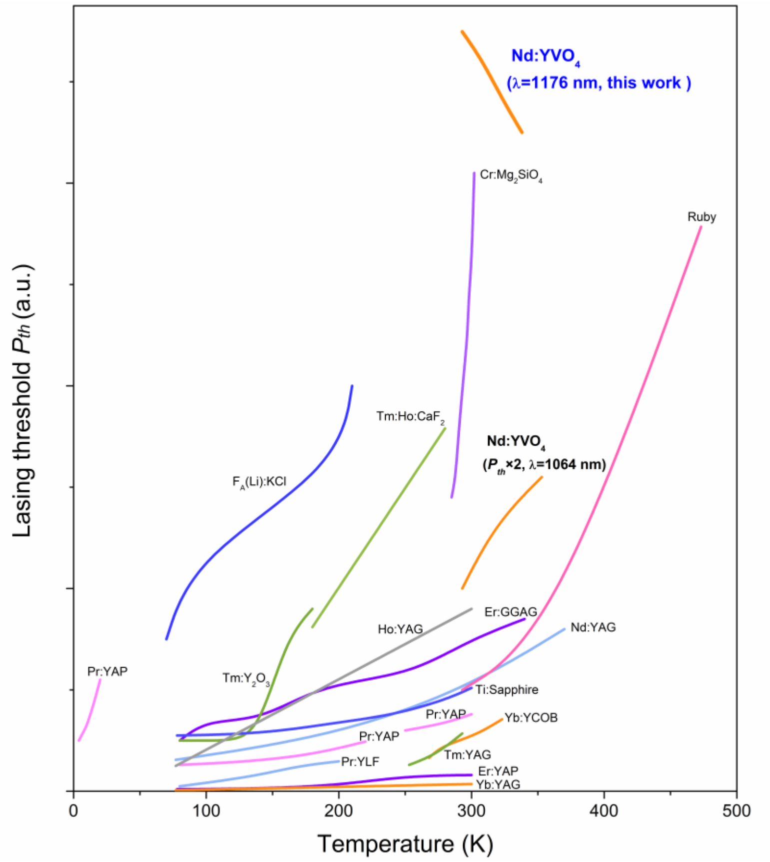

Figure R1. A summary of temperature dependent lasing threshold in solid-state lasers.

Action:

In the revision, we added "In previous reports, to the best of our knowledge, almost all solid-state lasers benefited from low temperature with the reduced P_{th} and increased slope efficiency, *e.g.*, ruby laser, Ti:sapphire, Yb:YAG, $Nd:YVO_4$ (A comprehensive summary is listed in the Supplementary Fig. S1 and Table S1)." In the Supplementary materials, Fig. R1 and Table R1 were added.

Table R1. A summary of temperature-dependent solid-state laser performances

Laser crystal	Temperature (K)	Threshold (a.u.)	Slope efficiency	References
Ruby λ ~ 0.694 μm	293 K	700 watts/cm^3	N/A	Journal of Applied Physics (1962), 33, 2333-2335.
	363 K	1100 watts/cm^3	N/A	
	473 K	3900 watts/cm^3	N/A	
F_A(Li) center in KCl λ ~ 2.7 μm	70 K	1.5 (a.u.)	N/A	Solid State Communications (1965), 3, 61-63.
	90 K	2.3 (a.u.)	N/A	
	200 K	3.2 (a.u.)	N/A	
	210 K	4.0 (a.u.)	N/A	
Co^{2+}:MgF_2 λ ~ 1.94 μm	80 K	6 mJ	15.9%	IEEE Journal of Quantum Electronics (1985), 21, 1582-1595.
	225 K	8 mJ	12.7%	
Ti:Sapphire λ ~ 0.75 μm	78 K	0.55 W	24%	Laser Physics (2018), 28, 085801.
	120 K	0.56 W	N/A	
	160 K	0.6 W	N/A	
	200 K	0.68 W	N/A	
	240 K	0.75 W	N/A	
	280 K	0.9 W	N/A	
	300 K	1.02 W	17%	
Cr^{4+}:Mg_2SiO_4 λ ~ 1.3 μm	285 K	2.9 W	N/A	IEEE Journal of Quantum Electronics (1998), 34, 1996-2005.
	288 K	3.1 W	N/A	
	290 K	3.5 W	N/A	
	294 K	4.1 W	N/A	
	297 K	4.5 W	N/A	
	298 K	4.9 W	N/A	
	300 K	5.2 W	N/A	
	302 K	6.1 W	N/A	
Cr^{4+}:YAG λ ~ 1.45 μm	276 K	1.08 W	42.1%	Journal of the Optical Society of America B (1995), 12, 930-937.
	293 K	1.215 W	34.2%	
Cr^{2+}:ZnSe λ ~ 2.2-2.4 μm	78 K	6 mJ	6.7%	Proc. SPIE (2019), 110330Y.
	180 K	6.5 mJ	6%	
	300 K	9 mJ	5.7%	
	380 K	15 mJ	3.4%	
Fe^{2+}:ZnSe λ ~ 3.98 μm	19 K	1.2 μJ	3.2%	Optics Letters (1999), 24, 1720-1722.
	70 K	3.0 μJ	1.7%	
Fe^{2+}:ZnSe λ ~ 4.54 μm	150 K	24.5 μJ	8.2%	Optics Letters (1999), 24, 1720-1722.
	170 K	46.3 μJ	5.2%	
Fe^{2+}:ZnSe λ ~ 4.1 μm	85 K	15 mJ	43%	IEEE Journal of Quantum Electronics, (2006), 42, 907-917.
	186 K	~ 35 mJ	~37%	
	220 K	~ 60 mJ	~28%	
Nd:YAG λ ~ 0.946 μm	243 K	50 J	10%	Applied Physics B (1991), 53, 6-10.
	248 K	50 J	10%	
	253 K	52 J	9.5%	
	263 K	57 J	9%	
	273 K	62 J	7%	
	283 K	70 J	6%	
	298 K	74 J	2%	
YAG/Nd:YAG/YAG composite rod λ ~ 0.946 μm	293 K	1.86 W	29%	Applied Optics (1998), 37, 5713-5719.
	298 K	1.92 W	27.8%	
	303 K	1.92 W	26.8%	
	308 K	2.1 W	23.5%	
	313 K	2.08 W	22%	
	318 K	2.13 W	20%	
	323 K	2.12 W	19%	
Nd:YAG λ ~ 1.06 μm	30 K	17.5 J	10%	Optics Communications (1989), 73, 62-66.
	77 K	14 J	NA	
	100 K	14.5 J	16.5%	
	150 K	16 J	NA	
	200 K	20 J	22%	
	250 K	21.5 J	NA	
	300 K	23 J	23%	
Nd:YAG λ ~ 1.0612 μm	77 K	0.31 (a.u.)	N/A	Journal of the Optical Society of America (1966), 56, 1409-1410.
	195 K	0.54 (a.u.)	N/A	
	295 K	1 (a.u.)	N/A	
	370 K	1.6 (a.u.)	N/A	
Cr:Nd:GSGG λ ~ 1 μm	213 K	4.88 J	N/A	IEEE Journal of Quantum Electronics (2003), 39, 741-748.
	233 K	5.02 J	N/A	

	253 K	5.17 J	N/A	
	273 K	5.35 J	N/A	
	293 K	5.55 J	N/A	
	313 K	5.78 J	N/A	
	333 K	6.04 J	N/A	
	353 K	6.34 J	N/A	
$Nd:YVO_4$ λ ~ 0.914 µm	278 K	NA	high	Jurnal Teknologi (Sciences & Engineering) (2016), 78, 149-154.
	333 K	NA	low	
$Nd:YVO_4$ λ ~ 1.064 µm	273 K	N/A	high	Appl. Opt. (1993), 32, 2085-2086
	373 K	N/A	low	
$Nd:YVO_4$ λ ~ 1.06 µm	293 K	1 W	N/A	Journal of the Optical Society of America B (2011), 28, 972-976.
	318 K	1.32 W	N/A	
	353 K	1.55 W	N/A	
$Nd:YVO_4$ λ ~ 1.342 µm	293 K	NA	good	Optics Communications (1999), 164, 191–197
	313 K	NA	poor	
$Nd:Y_2O_3$ λ ~ 1.073 µm	77 K	0.34 (a.u.)	N/A	Journal of the Optical Society of America (1966), 56, 1409-1410.
	195 K	0.64 (a.u.)	N/A	
	295 K	1 (a.u.)	N/A	
	370 K	1.78 (a.u.)	N/A	
$Nd:LaSc_3(BO_3)_4$ λ ~ 1.062 µm	77 K	~ 38 mW	44%	Applied Physics B Lasers and Optics, (1994), 58, 381-388.
	300 K	~ 40 mW	38%	
Yb:YAG λ ~ 1.03 µm	77 K	~ 9 mW	67%	Optics Letters, (1991), 16, 1089-1091.
	300 K	71 mW	~43%	
Yb:GGAG λ ~ 1.026 µm	100 K	2.5 mJ	36%	Proc. SPIE, High-Power, High-Energy, and High-Intensity Laser Technology III, (2017), 1023812
	200 K	4.3 mJ	31%	
	300 K	12.6 mJ	11%	
$Yb:Y_{0.77}Gd_{0.09}Ca_4O(BO_3)_3$ λ ~ 1.084 µm	268 K	0.33 W	60%	Optics Communication (2018), 427, 244-249.
	278 K	~ 0.45 W	58%	
	303 K	~ 0.55 W	55%	
	323 K	0.71 W	51%	
Yb: $YCa_4O(BO_3)_3$ λ ~ 1.023 µm	278 K	3.7 W	24%	Optics & Laser Technology (2018), 108, 360-363.
	323 K	6.75 W	20%	
Tm:YAG λ ~ 2.013 µm	253 K	0.26 W	44%	Optics Express (1999), 4, 12-18.
	273 K	0.36 W	34%	
	293 K	0.57 W	27%	
$Tm:Y_2O_3$ λ ~ 1.932 µm	80 K	0.5 W	32.2%	Applied Physics B (2020), 126, 44
	100 K	0.5 W	29.7%	
	120 K	0.5 W	26.5%	
	140 K	0.6 W	22.6%	
	160 K	1.5 W	21.6%	
	180 K	1.8 W	18.7%	
$Tm:GdVO_4$ λ ~ 1.84 µm	78 K	1 W	44%	Optica High-brightness Sources and Light-driven Interactions Congress 2022, Technical Digest Series (2022), paper JW5A.14.
	200 K	2.1 W	12%	
$Tm:Lu:CaF_2$ λ ~ 1.86 µm	78 K	1 W	65.5%	Journal of Luminescence (2023), 255, 119563
	200 K	1.2 W	55.9%	
	300 K	1.2 W	38%	
Ho:YAG λ ~ 2.097 µm	77 K	0.25 W	43%	Proceedings of SPIE (2009), 71931H.
	300 K	1.8 W	28%	
Ho:YLF λ ~ 2.055 µm	77 K	45 mW	28%	Applied Physics B (1994), 58, 69-71.
	210 K	80 mW	18%	
$Tm:Ho:CaF_2$ λ ~ 2.1 µm	180 K	1.62 W	15.7%	Advanced Solid State Lasers, (2014), paper ATh2A.14.
	280 K	3.58 W	8.6%	
Tm:Ho:YLF λ ~ 2.065 µm	100 K	~ 230 mW	N/A	Chinese Optics Letters (2003), 1, 281-282.
	170 K	~ 320 mW	N/A	
	200 K	~ 460 mW	N/A	
	220 K	~ 750 mW	N/A	
Pr:YLF λ ~ 0.607 µm	80 K	49 mW	46%	Laser Phys. Lett. (2015), 12, 095801
	110 K	100 mW	44%	
	140 K	160 mW	42%	
	170 K	250 mW	40%	
	200 K	295 mW	36%	
Pr:YAP λ ~ 0.493 µm	4 K	500 mW	26%	Applied Physics B (2021) 127, 2
	8 K	600 mW	N/A	
	10 K	650 mW	N/A	
	15 K	850 mW	N/A	
	20 K	1100 mW	N/A	
Pr:YAP λ ~ 0.622 µm	80 K	260 mW	13.5%	Laser Phys. Lett. (2014), 11, 105801
	130 K	290 mW	10.4%	
	180 K	360 mW	4.9%	
	220 K	490 mW	2.6%	
Pr:YAP λ ~ 0.662 µm	250 K	600 mW	13.4%	Laser Phys. Lett. (2014), 11, 105801
	280 K	670 mW	10.5%	
	300 K	760 mW	7.9%	
Pr:YAP λ ~ 0.747 µm	80 K	330 mW	55.1%	Laser Phys. Lett. (2014), 11, 105801
	130 K	360 mW	50.9%	
$Er:CaF_2$ λ ~ 2.7 µm	80 K	24 mW	2.3%	Proc. SPIE, Solid State Lasers XXIV: Technology and Devices, (2015), 93421S
	180 K	135 mW	2%	

	280 K	183 mW	1.3%	
Er:YLF λ ~ 2.8 μm	80 K	2 mJ	22.8%	Proc. SPIE, Solid State Lasers XXVIII: Technology and Devices, (2019), 108961L
	100 K	2 mJ	20.7%	
	300 K	5 mJ	16.4%	
Er:GGAG λ ~ 1.6 μm	80 K	0.5 W	54%	Opt. Mater. Express (2020), 10, 1249-1254
	100 K	0.7 W	52%	
	140 K	0.7 W	52%	
	180 K	1 W	51%	
	220 K	1.1 W	45%	
	260 K	1.2 W	41%	
	300 K	1.5 W	37%	
	340 K	1.7 W	29%	
Er:GGAG λ ~ 2.92 μm	80 K	16 mJ	9.9%	Proc. SPIE 11259, Solid State Lasers XXIX: Technology and Devices, (2020), 112591Q
	100 K	15 mJ	8.7%	
	200 K	15 mJ	7.6%	
	300 K	17 mJ	6.4%	
Er:Pr:GGAG λ ~ 2.9 μm	80 K	210 mW	16%	Proceedings Volume 11980, Solid State Lasers XXXI: Technology and Devices; (2022), 119800A
	100 K	250 mW	12%	
	300 K	270 mW	6%	
Er:YAP λ ~ 2.7 μm	78 K	0.02 W	1.27%	Proc. SPIE, Solid State Lasers XXVII: Technology and Devices, (2018), 1051121
	100 K	0.02 W	1.26%	
	150 K	0.03 W	1.07%	
	200 K	0.06 W	0.79%	
	250 K	0.15 W	0.31%	
	300 K	0.16 W	0.14%	

Comment:

2. *The novelty of the work must be elaborated in the introduction to provide better understanding to the readers.*

Response:

Thank you for your comments. We emphasized the significance of "phonon pumping" in the revision. This is the biggest highlight of this work. And it can be supported by the experimental results. As shown in Fig. R2, when the photon pumped power maintains constant, there exists a phase transformation from 1064 nm to 1176 nm lasing with increasing temperatures. The phonon pumping is related to the temperature T_{th} in the critical region.

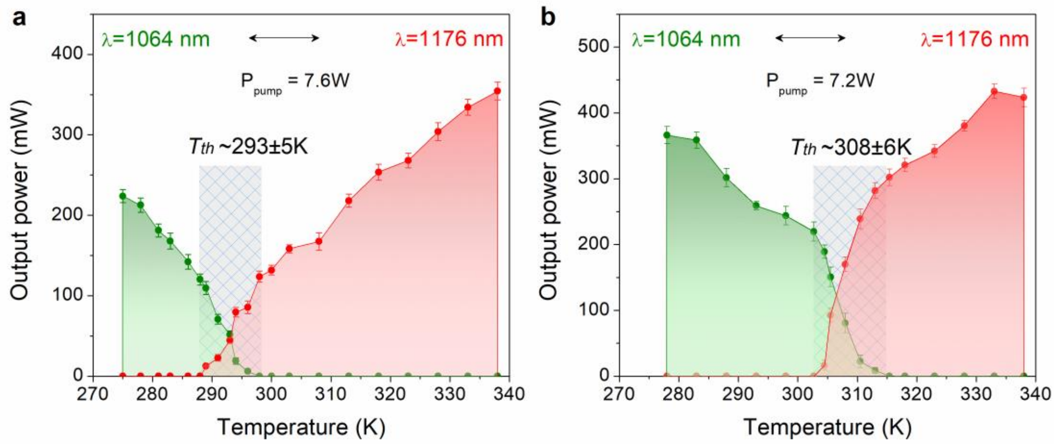

Figure R2. Phase diagram of 1064 and 1176 nm lasing under different pump powers.

First, the phonon-free 1064 nm laser is dominated at low temperature. Then, the output power of 1064 nm becomes deteriorated, and the phonon-pumped 1176 nm laser gradually excels it with increasing temperature. When photon-pumped power maintains 7.6 W, there exists a critical transition from 1064 nm to 1176 nm lasing around 293 K. The phonon pumping is related to the temperature T_{th} in the critical region. Below T_{th}, only the ZPL 1064 nm laser appears due to insufficient phonon supply. Beyond T_{th}, the phonon-pumped laser at 1176 nm starts to appear and become stronger and stronger, associated with the coherent phonons in the system. In addition, this temperature threshold T_{th} is dependent on the input power. As shown in Fig. R2b, the temperature threshold T_{th} will increase to around 308 K with a low photon-pumped power of 7.2 W, because the 1176 nm laser needs more supplied phonons in this case. Moreover, the output power of the 1176 nm laser tends to be saturated at high temperature, and earlier upon the lower input photon power.

Action:

The significance of this work has been emphasized in the revision. Fig. R2 was added in the revised Fig. 4.

Comment:

3. *At many instances, authors have used catch words like "brand-new"; "smoking gun evidence" etc. These should be toned to scientific language like "novel"; "conclusive evidence" to avoid over exaggeration.*

Response:

Thank you for your comments. We have changed these catch words by some scientific words.

Please see "Such a ~~brand-new~~ novel laser provides us an extra and conveniently degree of freedom."

"Another ~~smoking-gun~~ conclusive evidence for our proposed photon-phonon collaborative mechanism is ……"

Comment:

4. *Authors must provide pump input dependent spectra under normalized condition instead of just the linewidths.*

Response:

We thank the reviewer for raising this crucial issue. We added the pump-dependent emission spectra at 293 K under the normalized condition in Fig. R3. We can see that the FWHM of the fluorescence spectrum is around 2 nm when $P_{pump} < P_{th}$, and the FWHM of laser spectrum decreases to about 0.1~0.2 nm when $P_{pump} > P_{th}$. This is consistent with laser theory. For other temperatures at 308 K, 323 K, and 338 K, the change trends of FWHMs are similar. We added them in the Supplementary Materials (Fig. S14-S17).

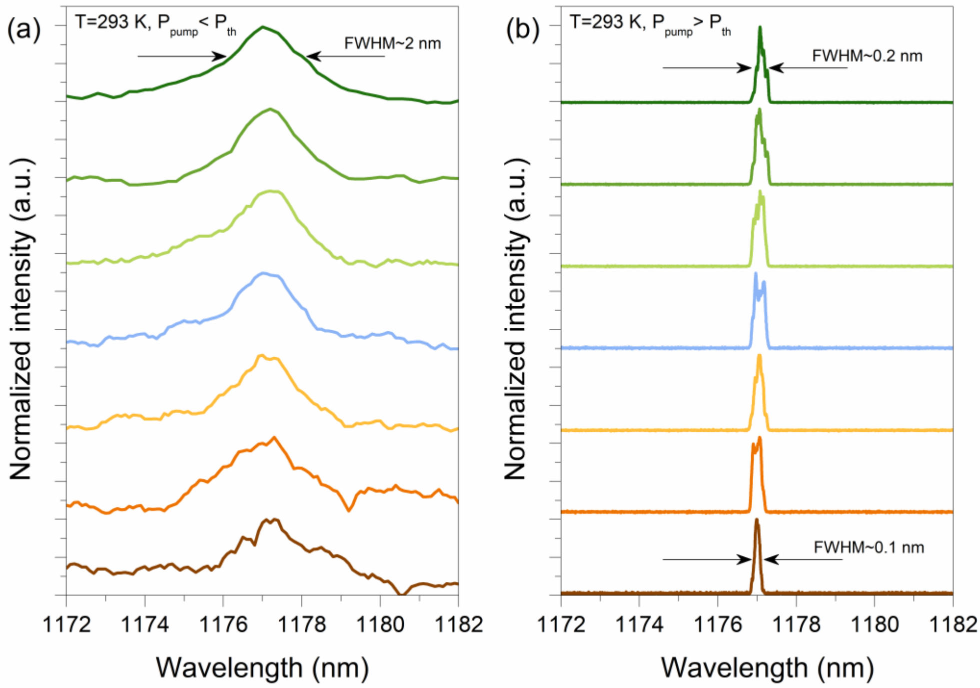

Figure R3. The pump dependent fluorescence and laser spectra under normalized condition, T=293 K. The resolution of the spectrometer for spectral measurement is 0.05 nm. With the increasing pump power, there are some multi-mode laser operations.

Action:

The pump dependent fluorescence and laser spectra at 293-338 K have been added in the revised Supplementary Materials, see Fig. S14-S17.

Comment:

5. What are the absolute input vs output slopes for lasers, below and above the threshold? These should be calculated through log-log plot of input vs output power/intensity.

Response:

Thank you for your suggestions. In general, the output power of a solid-state laser obeys the rule, $P_{out} = \eta_{\text{slope}} \times (P_{pump} - P_{th})$. Therefore, we used a linear plot to obtain a slope efficiency η.

In addition, according to the reviewer's suggestion, we also plotted the log-log graph for input power versus output power in Fig. R4. However, we think the slope in the *log-log* plot doesn't give helpful information because our laser is a direct lasing process but not a high-order nonlinear optical process or lasing in microcavity [ref]. When our lasing is operating in $Nd:YVO_4$ crystal beyond the threshold, its intensity is greatly overwhelmed with respect to weak fluorescence (>10^4 times). This also differs from microcavity lasing, where laser intensity beyond the threshold is only $10 \sim 10^2$ times of fluorescence intensity. Therefore, we still prefer linear plots.

[Ref]: Liang, Q., et al. "Circularly polarized lasing from a microcavity filled with achiral single-crystalline micro-ribbons." *Angew Chem Int Ed*, (2022), DOI:10.1002/anie.202213229, *log-log* plot in Fig. 3c & 3f.

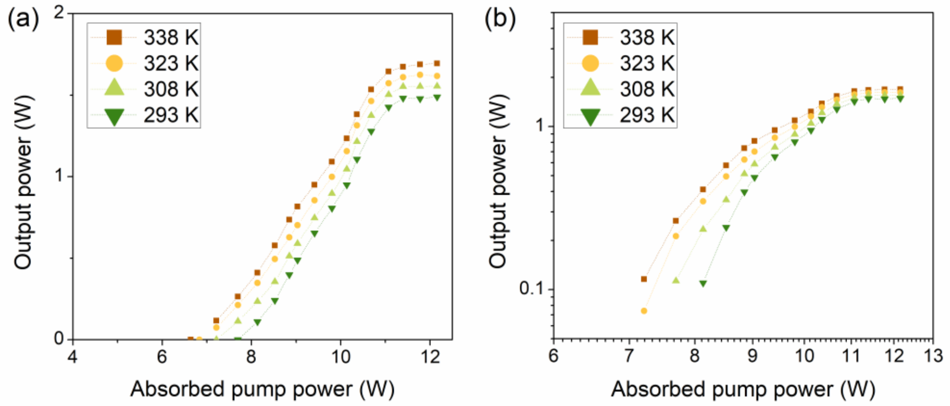

Figure R4. Input power versus output power of $Nd:YVO_4$ crystal. **a.** linear plot, **b.** log-log plot.

Comment:

6. For polarization measurement, authors should clarify the degree of polarization using maximum and minimum intensities of the non-normalized data, spectral data should also be provided.

Response:

Thanks for your suggestions. We give non-normalized polarization data in Fig. R5a. We can see that the maximum and minimum laser powers after Glan-Taylor polarizer are 268.3 and 0.036 mW, respectively. So, the degree of polarization (ρ) is 99.97% by the formula of $\rho = \frac{I_{//} - I_{\perp}}{I_{//} + I_{\perp}}$, where $I_{//}$ is the intensity of light parallel to the polarizer, and $I_{\perp}$ is the intensity of light perpendicular to the polarizer [Ref: *Appl. Phys. Lett.* 105, 031111 (2014)]. The spectral data are plotted in Fig. R5b. This result indicates our laser is a near-perfect linear-polarized light.

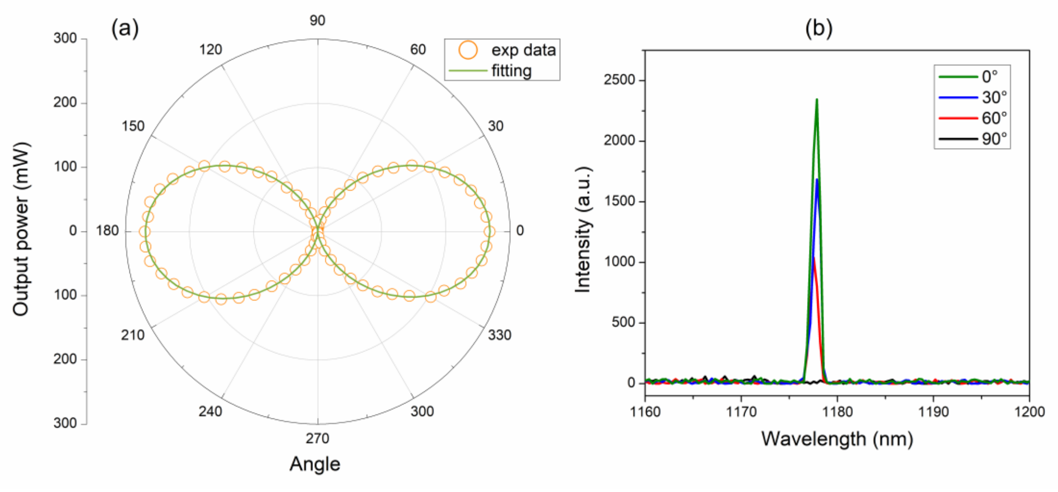

Figure R5. **a.** Polarization measurement of 1176 nm laser. **b.** Laser spectra for various polarization angles.

Action:

Fig. R5 has been added in the revised supplementary materials, see Fig. S18.

Comment:

7. What are beam quality factors at different temperatures? How does the crystal dimensions and cavity parameters impact the phonon assisted photon laser characteristics? How much was the beam spot size and beam divergence in mrad?

Response:

We thank the reviewer for raising this critical issue. The beam profiles at 293 K have been added in Fig. R6. For other temperatures and configurations (crystal dimensions and cavity lengths), the beam profiles have been added in Figs. S20-S26. The beam quality at 293, 308, 323, and 338 K were calculated in Fig. R7. All beam qualities and beam divergences are measured while the output power maintains 1 W.

We can see from Table R2, for the crystal with a dimension of 3×3×7.6 mm^3 and the cavity with a R_{oc} = 50 mm output coupler, the largest M_x^2 and M_y^2 are 2.35 and 3.58, respectively. The beam quality at low cooling temperature is better than that at high temperature. And the temperature has no significant effect on the divergence angle of the photon-phonon co-pumped laser in our experiment.

For the cavity with a R_{oc} = 100 mm output coupler, at the cooling temperature of 338 K, M_x^2 and M_y^2 are 1.84 and 1.95, respectively. It has a better laser characteristic compared to the result of the cavity with R_{oc} = 50 mm output coupler, including a smaller M^2 factor and a smaller beam divergence. However, it requires higher pumped power to achieve a 1 W photon-phonon pumped laser.

For the crystal with a small dimension of 2×2×7.4 mm^3, its beam quality and divergence angle are basically the same as that of 3×3×7.6 mm^3 at the same temperature. Therefore, crystal size is not a crucial factor for our phonon-pumped laser.

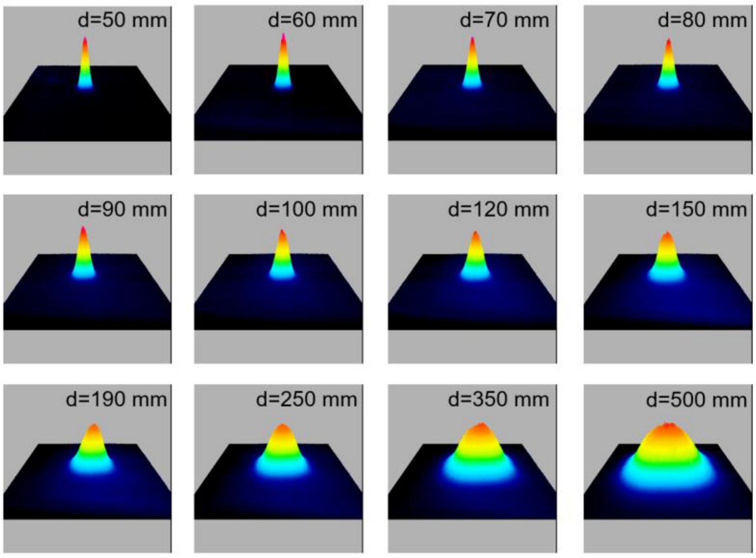

Figure R6. Output beam profiles of 1176 nm laser at 293 K. The output power maintains 1 W. Cavity length (R = 50 mm). *d* represents the distance between output coupler and CCD detector.

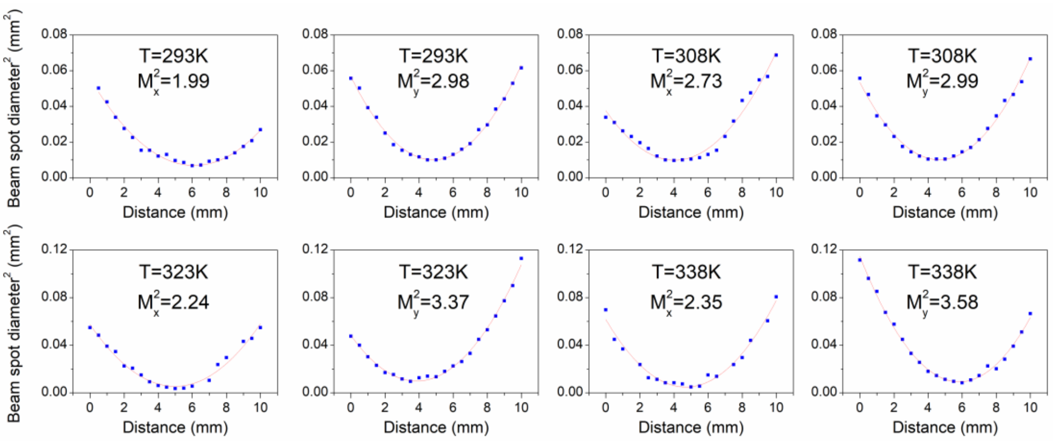

Figure R7. Beam spot radius as a function of distance measured at a crystal temperature of 20-65 °C. R_{oc}= 50 mm.

Table R2. Beam quality parameters of 1176 nm laser at different temperatures.

$Nd:YVO_4$ crystal size and cavity length	Water-cooling temperature (K)	M_x^2	M_y^2	Beam spot radius (μm)	Beam divergence (mrad)
3×3×7.6 mm^3 plane-concave (R_{oc} = 50 mm)	293	1.99	2.98	63.36	5.91
	308	2.73	2.99	62.42	6.0
	323	2.24	3.37	60.46	6.19
	338	2.35	3.58	62.58	5.98
3×3×7.6 mm^3 plane-concave (R_{oc} = 100 mm)	338	1.84	1.95	99.65	3.76
2×2×7.4 mm^3 plane-concave (R_{oc} = 50 mm)	338	3.28	2.65	76.65	4.88

Action:

All these figures and tables have been added in the revised Supplementary Materials.

Reviewer #2

Comment:

The authors claim a new type of laser that is collaboratively pumped with both photons and phonons. They present data that shows a conventional power threshold and input-output characteristic for a Nd:YVO$_4$, laser operating at 1176 nm. The laser also shows an unusual temperature threshold for laser action- i.e. above a critical temperature at constant pump power the laser increases its output with increasing temperature.

While this is presented as phonon pumping, I do not think that this is an accurate description of the process. The laser is pumped to the $^4F_{3/2}$ level solely by the 808 nm pump photons.

Response:

We thank the reviewer for his/her detailed and constructive comments.

We agree that the laser is pumped to the $^4F_{3/2}$ level by the 808 nm laser diode, but its experimental setup is very different from previous Nd:YVO$_4$ lasers at 1064 nm. Here, we must emphasize that our laser differs from conventional Nd:YVO$_4$ laser, generated by the transitions between different electronic levels. The energy levels responsible for the present laser are generated by the electron-phonon coupling, corresponding to a novel phonon-pumping mechanism and an anomalous temperature dependent lasing threshold behavior. In addition, a critical temperature threshold was discovered for 1176 nm laser generation.

(1) In previous solid-state lasers, no matter vibronic or non-vibronic lasers, the lasing threshold (P_{th}) exhibits a positive temperature dependence of $\partial P_{th}/\partial T>0$ (see Fig. R1). In this work, we proposed a new-type phonon-pumping mechanism whose lasing threshold has an anomalous temperature behavior with $\partial P_{th}/\partial T<0$. This phonon-pumped laser prefers heat and has a better performance without external cooling. We consider this finding is a significant breakthrough innovation for laser physics and technology.

(2) We experimentally verified this novel phonon-pumping mechanism on Nd:YVO$_4$ crystal. In previous studies, Nd:YVO$_4$ was not considered as a vibronic laser crystal owing to its extremely weak electron-phonon coupling effect, and it mainly had four discrete lasing wavelengths at 914, 1064, 1086, and 1342 nm. Our experimental results broke this limitation and demonstrated that Nd^{3+} ion also holds interesting electron-phonon coupling and vibronic lasing behaviors. It exhibits a negative temperature dependence of $\partial P_{th}/\partial T<0$ in the 295-338 K range.

(3) We gave a power-temperature transition diagram between phonon-free 1064 nm and phonon-pumped 1176 nm laser (Fig. R8). A distinct temperature threshold T_{th} was observed. That is, only at a sufficiently high temperature, the 1176 nm laser can appear. Similar to threshold P_{th} in photon pumping, this critical temperature T_{th} is a manifestation of phonon pumping. Meanwhile, the threshold-temperature phase diagram of the present laser is theoretically revealed and experimentally verified with a general threshold curve ruled by $P_{th} = C/T_{th}$ (constant C upon loss), similar to Curie's Law which describes the relationship between the magnetic susceptibility of a paramagnetic substance and its thermodynamic temperature.

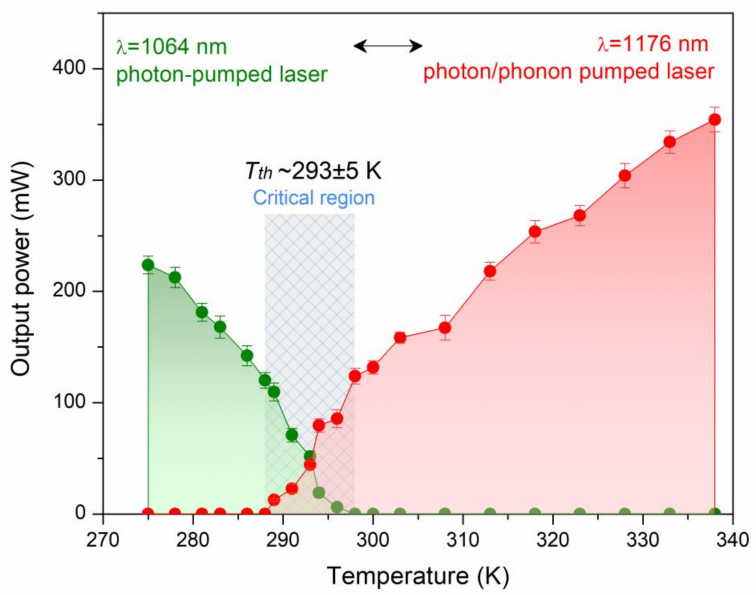

Figure R8. Power-temperature transition diagram of 1064 and 1176 nm laser. The critical region represents the emergence of phonon-pumping process. T_{th} is a temperature threshold for phonon-pumped lasing.

Action:

The revised version emphasizes the phonon-pumping mechanism. Some new results are added in Fig. 4.

Comment:

An increasing temperature does indeed increase the oscillator strength of a weakly emissive transition at 1176 nm. This appears to arise from a thermal change in the normal coordinates of the system, giving an improved wavefunction overlap of initial and final state for the relevant transition. This unusual phenomenon has the effect of increasing the stimulated emission cross-section with temperature. If the phonons were however to be pumping the laser, one would expect a change in the population inversion. I therefore think that the authors need to modify the way in which they are presenting their results.

Response:

We thank the reviewer's comments. We agree with the comment about the thermal change in the normal coordinates, giving an improved wavefunction overlap of the initial and final states for the relevant transition, and increasing the stimulated emission cross-section with temperature. But the phonon pumping also changes the population inversion, which is not contradictory to traditional population inversion. Our laser is a synergetic photon-phonon pumping process by input pump power and high temperature simultaneously.

As shown in Fig. R9, for a conventional lasing at 1064 nm, the population inversion happens between 0'' and 0' state. Owing to a large energy difference ΔE (ground state→0'), the population $n_{0'}$ is usually considered as zero. So, it is easy to obtain a population revision ($n_{0''} > n_{0'}$) by sufficient photon pumping ($W_{G\to E} \propto P$) and fast relaxation from the excited state to 0'', then hence realize lasing at 1064 nm.

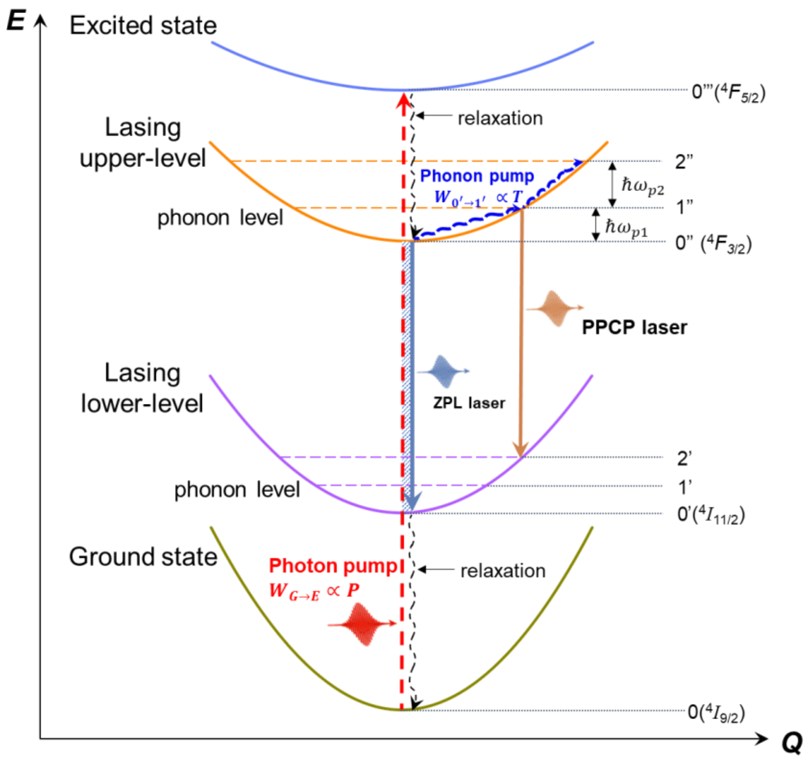

Figure R9. Configurational coordination model for phonon-pumped lasing.

For our photon-phonon pumped laser, the population inversion should happen between 1" and 2' state ($n_{1''} > n_{2'}$ for lasing), according to the description of the electron-phonon coupling and four-level model of lasers [Ref: Richard C. Powell, *Physics of Solid-State Laser Materials*, 1997, AIP Press], which both lasing upper and lower levels are coupled to phonon vibrations. The first step, in photon-pumping process, a large population $n_{0''}$ is realized. However, this is not sufficient for 1176 nm. There must be a second phonon-pumping step from 0" to 1", and a population inversion happens between 1" and 2' states. This pumping rate is determined by the temperature ($W_{0''\rightarrow 1''} \propto T$), because the phonon occupation numbers n_p are given by the Bose-Einstein distribution function,

$$n_p = \frac{1}{e^{\hbar w_p / k_B T} - 1}$$

where $\hbar$ is Planck constant, w_p is phonon frequency, k_B is Boltzmann's constant, and T is the temperature. A higher T, a larger n_p will be. If temperature is too low (small $W_{0''\rightarrow 1''}$), the population of 1" would not be large enough to make population inversion ($n_{1''} < n_{2'}$), and the lasing at 1176 nm is not allowed. If the temperature is very high, a two-phonon pumping (0" → 2") process can also be expected (*e.g.*, 1231 nm lasing observed in Nd:YVO_4 crystal). Therefore, there is actually a synergetic photon-phonon pumping process in our proposed new lasing mechanism.

Action:

We have corrected the written format in the revision, see Fig. 1a and Page 3-4. All above analysis has been added in the revised Supplementary Materials.

Comment:

The authors argue that a major limitation of solid-state lasers is the strong thermal effects that can affect their *operation under intense optical pumping. This is certainly true, although the main thermal issues that arise are effects of thermal lensing and possible physical damage to the crystal. For three-level lasers or quasi-three-level laser systems thermal effects can reduce the population inversion and hence the material gain, but this is largely not an issue for four-level laser media, as is presented here. The phenomenon described in this manuscript does not appear to address these thermal problems.*

Response:

Thanks for your comments. We agree that the thermal effect is crucial in three-level lasers or quasi-three-level laser systems, *e.g.*, ruby laser and Yb:YAG laser, due to the temperature-dependent populations of electrons at lower levels. However, the thermal effect is also a crucial problem for four-energy levels (*e.g.*, Nd^{3+} ion) because their laser performances also deteriorated with increasing temperature (see Fig. R1 and Table R1).

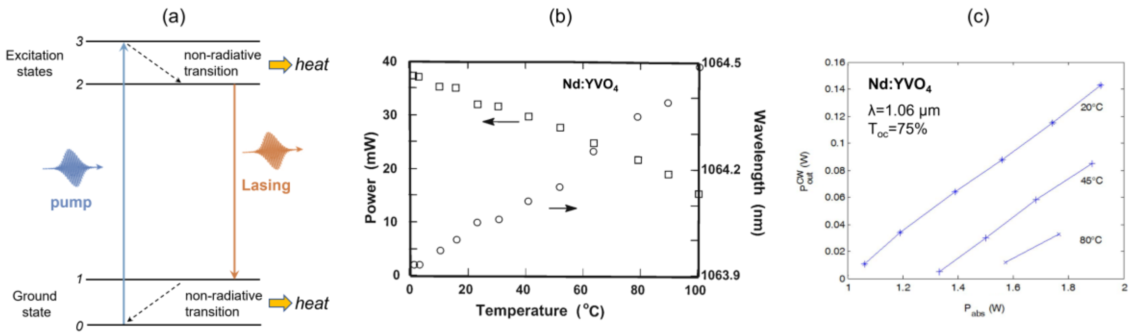

Figure R10. (a) Schematic of a four-level Nd^{3+} laser system, (b) Temperature-dependent laser performances of Nd:YVO_4 at 1064 nm. [*Ref: G. C. Bowkett (1999). Nd:YVO_4 microchip lasers and amplifiers, School of Communication & Informatics, Victoria University of Technology, PhD thesis. Page 118, Figure 5.4*; *Appl. Opt. (1993), 32, 2085-2086*], (c) Temperature-dependent laser performances of Nd:YVO_4 at 1064 nm. [*Ref: Journal of the Optical Society of America B (2011), 28, 972-976*]

A typical four-level Nd^{3+}-laser system is depicted in Fig. R10(a). In the presence of pumping light, the electrons on the ground state will be excited to the top one, then rapidly relaxed to the lower level 2 with non-radiative transitions. After the laser transition to terminal level 1, there exists another non-radiative transition between level 1 and ground level 0. Thus, two non-radiative transition processes brought serious thermal problems in traditional four-level laser systems. In laser theory, the population of level 1 can be considered as zero (large ΔE between 0 and 1). Therefore, if we don't consider electron-phonon coupling effect and thermally induced cross-relaxation, heat is not a big issue in Nd^{3+}-lasers because the population of level 1 was nearly independent on crystal temperature. As a result, the fluorescence lifetime and hence the power performance are quite insensitive to variations in temperature [*refs: Opt. Commun. (1999), 164, 191-197*].

However, if the electron-phonon coupling effect was involved in the lasing process, the thermal effect would also be a great issue for four-level systems. With the increasing temperature, the electron-phonon coupling effect can modulate the energy transfer between electronic transition and lattice vibrations, thus leading to an inevitable influence on the population of phonon-involved levels (Fig. R9). Therefore, thermal effect is an important topic in both three-level and four-level laser systems. In previous reports, the output power of Nd:YVO_4 microchip lasers at 1064 nm decreased with increasing temperature from 0 to 100 °C, which is common for solid-state lasers. In addition, the lasing thresholds also increased at high temperatures (Fig. R10).

In our work, we realized a thermally-enhanced 1176 nm laser with the assistance of hot phonons, where the temperature does change not only the stimulated emission cross-section but also the population inversion. This is a great novelty for laser physics.

Action:

We added a section "thermal effect in a four-energy level laser system" in the Supplementary Materials, see Page S32.

Comment:

I have a number of other smaller specific comments on the details of the paper which I enumerate below.

1. Line 17: should be "Cooper pairs".

Response:

We are sorry for this typo. We have corrected it in the revision.

Comment:

2. Line 19: the word "preferring" should be replaced with a more technical term.

Response:

Thank you for your suggestion. We changed "preferring" to "make stronger by heat".

Comment:

3. Line 32: the phrase "spontaneously generate" should be rephrased.

Response:

We changed "spontaneously generate" to "laser will be created when pump power beyond a threshold (P_{th}) overcomes the critical loss."

Comment:

4. Line 43: I am not sure what this sentence means.

Response:

Line 43, "For example, the accessible wavelengths upon intrinsic energy levels of doping ion and the P_{th} upon *gain coefficient* of materials are already determined for a given laser crystal."

We changed "critical loss" to "gain coefficient".

Comment:

5. Line 64. The authors state that "by selecting and amplifying specific-symmetry phonons,…" This does not appear to be an accurate description of what the paper shows.

Response:

In the revised Fig. 4b, we added a laser wavelength at 1168 nm by amplifying another specific-symmetry E_{g} phonons (Fig. R11). It can also be explained by our proposed selection rules.

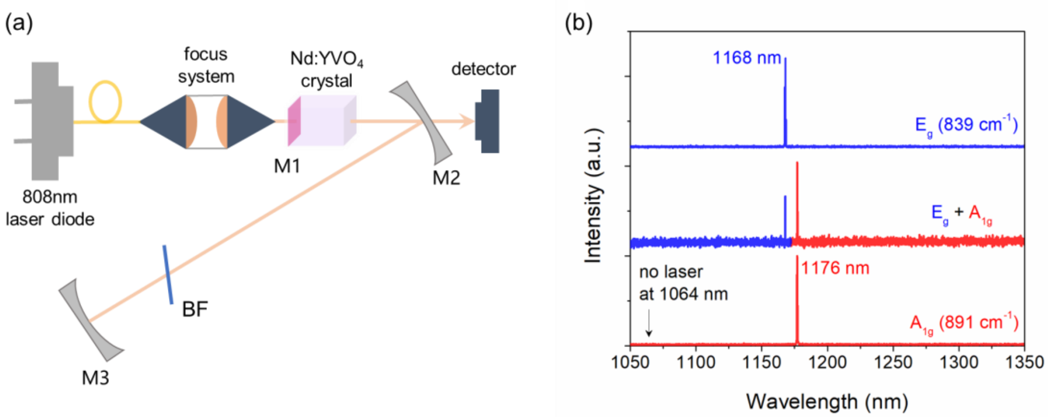

Figure R11. Tunable phonon-pumped laser in one-phonon process. In a V-shape cavity, via rotating Bf plate and adjusting the intracavity loss, we can obtain the strongest 1176 nm laser coupled to A_{1g} mode, and the second-strongest 1168 nm laser coupled to E_g mode. In addition, these two laser wavelengths can be co-existed at a special angle of the BF plate.

Comment:

6. Line 82: this sentence should be rephrased in more scientific language.

Response:

Line 82, "However, fantastic phenomena will happen in the lasing resonant cavity even for this extremely weak coupling, e.g., three orders of magnitude smaller."

We changed this sentence: However, strong phonon-pumped laser still be obtainable in the lasing resonant cavity even for this extremely weak coupling, e.g., three orders of magnitude smaller."

Comment:

7. Line 83: The authors refer to "Those virtual levels become solid…", however, it is clear for photoluminescence measurements the transition to these levels is allowed (there is weak photoluminescence at all temperatures) and so these are probably not virtual levels.

Response:

In the revision, we used a configurational model to describe phonon-pumping effect. All "virtual levels" have been deleted. The stimulated transition happens between the electronic levels coupled with specific phonons.

Comment:

8. Line 106: The equation on line 106 appears to claim that the photon energy is proportional to the threshold temperature, which cannot be correct.

Response:

Thank you very much for this suggestion. This formula is not clear and we have deleted it.

Comment:

9. Line 137: the authors refer to a step in the Huang-Rhys factor near 400 K, "…implying some unusual physical appearances" – this seems rather speculative and unsupported.

Response:

We changed this expression. There is a step in the Huang-Rhys factor near 400 K, which is related to the strongly strengthened electron-phonon coupling effect.

<u>Comment:</u>

10. Line 207: the sentence does not make sense and should be clarified.

<u>Response:</u>

Line 207, "Before lasing, the lower phonons (temperature) naturally require more collaborative photons to overcome loss, leading to a higher P_{th}."

We changed this expression.

"When the temperature is low, phonon number is small, leading to a less contribution to the laser gain in the system. The laser gain mainly depends on the photon pumping in this condition. Therefore, it requires higher photon-pumped power to generate a photon-phonon collaborative pumped laser at low temperature."

<u>Comment:</u>

11. Line 230: I do not think it is obvious that "T_{slope} will increase with higher saturation output power at a higher pump power." The authors should explain/justify this more clearly.

<u>Response:</u>

We changed the expression of this sentence. Please see "It is expected that the temperature-dependent saturation output power will increase at a higher pump power."

<u>Comment:</u>

12. Line 242: Equation 3 suggests that the population inversion increases linearly with time – is this what the authors intend to state? I thought that it would be better to solve the relevant rate equation for the steady-state condition, rather than present a transient phenomenon that assumes that the transition lifetime is much greater than t.

<u>Response:</u>

We give a steady-state equation for our laser. The temperature-dependent behavior of PPCP laser can be described by the coupled rate equations. For our phonon-involved four-level system, the rate equations can be written as,

$$\frac{dn_{0'''}}{dt} = n_0 W_{00'''} - n_{0'''}(S_{0'''0''} + A_{0'''0})$$

$$\frac{dn_{0''}}{dt} = -n_{0''} W_{0''2'} - n_{0''} A_{0''2'} + n_{0'''} S_{0'''0''} - n_{0''} S_{0''1''}$$

$$\frac{dn_{1''}}{dt} = n_{0''} S_{0''1''} - n_{1''} W_{1''2'} - n_{1''} A_{1''2'}$$

$$\frac{dn_{2'}}{dt} = n_{0''} W_{0''2'} + n_{0''} A_{0''2'} - n_{2'} S_{2'0} + n_{1''} W_{1''2'} + n_{1''} A_{1''2'}$$

$$\frac{dn_0}{dt} = n_{2'} S_{2'0} - n_0 W_{00'''} + n_{0'''} A_{0'''0}$$

where n_i represents the electron population densities of level i, W_{ij} is the transition probability for stimulated radiation between level i and j, A_{ij} is the spontaneous transition probability, and S_{ij} is the nonradiative transition probability. Considering the probability of nonradiative transition $S_{0'''0''}$ is much larger than spontaneous emission probability $A_{0'''0}$, and assuming a steady-state condition, $dn_{0'''}/dt=0$, we can obtain

$$n_0 W_{00'''} = n_{0'''} W_{0'''0''} = W_p$$

where W_p is pump rate.

For the case of thermal equilibrium, the relative populations of level 1" and phonon-pumped level 0" is determined by the Boltzmann distribution,

$$\frac{n_{1"}}{n_{0"}} = e^{-\frac{E_{1"}-E_{0"}}{k_B T}}$$

where $E_{1''}$-$E_{0''}$ is the energy separation between level 1" and 0", k_B is Boltzmann's constant, T is temperature. Considering $dn_{1''}/dt= dn_{0''}/dt =0$, we can obtain the population inversion Δn as follows

$$\Delta n = n_{1"} - n_{2'} = \frac{W_p\left[S_{2'0} - e^{\frac{E_{1"}-E_{0"}}{k_B T}}\left(W_{0"2'} + A_{0"2'}\right) - \left(W_{1"2'} + A_{1"2'}\right)\right]}{\left[e^{\frac{E_{1"}-E_{0"}}{k_B T}}\left(2S_{0"1"} + W_{0"2'} + A_{0"2'}\right) - \left(W_{1"2'} + A_{1"2'}\right)\right]S_{2'0}}$$

It clearly shows the relationship between population inversion and temperature. Higher temperature T is helpful for the formation of population inversion. At the condition of steady state, the population inversion stabilized and the electron population densities at each level keep unchanged with time. However, before the creation of population inversion, population inversion would change with time, thus our model is suitable for this condition.

Comment:

13. Line 247: the authors introduce a relationship that the emission cross-section is proportional to temperature. This may be approximately found in the empirical fluorescence data, but it is not clear that this is generally true.

Response:

We explained this expression in the Supplementary Materials, see Page S37.

Comment:

14. Line 263: what is meant by "...the uncooling conditions..."?.

Response:

"The uncooling conditions" means an experimental condition that external water-cooling was removed from Nd:YVO_4 crystal.

Comment:

15. Line 266: should the equation include the term (beta / P_{th})?

Response:

Equation (9) don not include the term beta / P_{th}, because P_{th} is only a critical value for lasing. The output power P_{out} is determined by the incident pump power P_{pump} in the photon-pumping process.

Comment:

16. Line 274: what is meant by "...without cooling situation"?

Response:

The "without cooling situation" means an experimental condition that external water-cooling was removed from Nd:YVO_4 crystal.

Comment:

17. Line 286: what is meant by "...a traditional yet newly introduced degree of freedom..."?

Response:

This sentence means that the temperature threshold, corresponding to phonon pumping, would be an important factor to modulate the laser performances. Therefore, we consider it as a new degree for laser physics.

Comment:

18. Line 293: I am not sure there is evidence presented in the manuscript to support the claim that the observed data could be deemed "…an emerging microscopic quantum phenomena like superconductors…"

Response:

We deleted this sentence. "~~…an emerging microscopic quantum phenomena like superconductors…~~"

Comment:

19. Line 296: I do not think there is a strong case presented for impact in the given areas of research that are claimed.

Response:

Line 296, "Our PPCP laser platform is ready for applications in many scenarios such as high-temperature tolerant laser equipment, quantum nanophotonic, entangled phonons generation, and laser therapy with new wavelengths".

Here, we provided a direct application for yellow laser generation by our phonon-pumped laser. Combining with intracavity nonlinear frequency doubling by LBO crystal, we obtained a visible yellow laser at 588 nm (Fig. R18). This compact yellow laser would be possible to apply to retina surgery and ophthalmology, since the oxygen-rich blood pigment, known as oxyhemoglobin, absorbs most strongly at this wavelength.

[Ref] Ophthalmic Surgery Lasers and Imaging Retina, (2012), 43(4), 341-347

Comment:

20. Line 389: What is the two-phonon pumping process mentioned here?

Response:

We are sorry for this typo. We have corrected this sentence to "the monolithic configuration was employed for laser generation."

Comment:

21. Line 415: the authors should describe in more detail the measurement of fluorescence as a function of temperature. What was the specific sample used for these measurements? What angular range of light collection was used, and was any precaution taken to confirm that the collection efficiency of fluorescence does not change with sample temperature?

Response:

We used an in-situ technique to measure the fluorescence. The crystal sample, detector angle, and collection efficiency maintain unchanged in experiments. Only the crystal temperature was changed.

Comment:

22. Figure 2: I think it would be helpful to add a graph of the emission cross-section versus temperature, and compare this with S versus temperature from the same temperature range as used in the laser measurements.

Response:

Thank you very much for this suggestion. We added a new graph in the revision, see Fig. R12. It is observed that both emission cross-sections and Huang-Rhys *S* factors have a step jump around 400 K. This jump indicates the significantly increased phonon numbers involved in the phonon-pumped emission. This graph has been added in the revised main text, Fig. 2d.

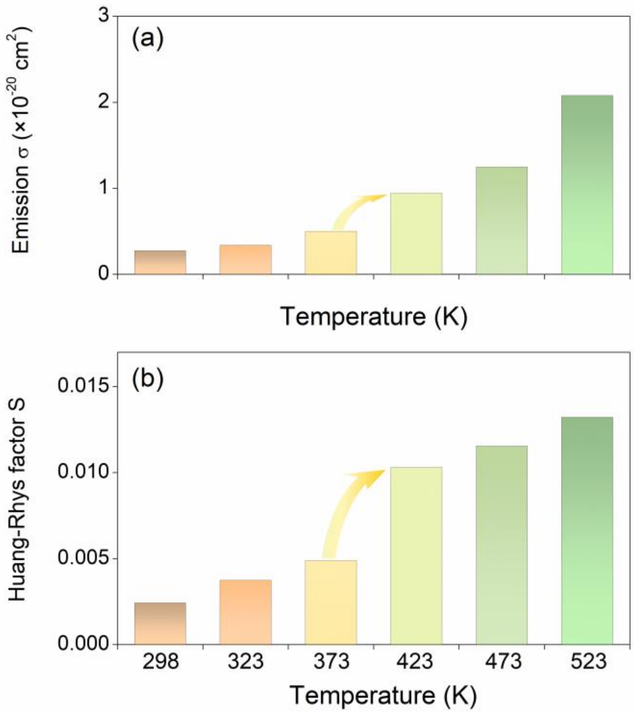

Figure R12. The emission cross-section (a) and the calculated Huang-Rhys *S* factors (b) at different temperatures.

Comment:

23. Supplementary Information page 23: the authors claim that the phonon energy is proportional to k_BT. However, if this were true, then surely the wavelength of the transition would change with temperature?

Response:

Thank you very much for this suggestion. First, this sentence should be "the total phonon energy is proportional to k_BT". We have corrected it.

Then, the laser wavelength is surely dependent on the temperature. We measured the laser wavelength under different temperatures. As shown in Fig. R13a, there are two lasing wavelengths, 1064 nm at low temperature and 1176 nm at high temperature. The transition temperature locates around 293-296 K. We found that there is a wavelength shift from 1176.5 to 1176.8 nm with increasing temperature from 296 to 338 K. This shift can be exactly explained by our proposed laser theory.

According to reference [G. C. Bowkett (1999). Nd:YVO_4 microchip lasers and amplifiers, Victoria University of Technology, PhD thesis. *Page* 118, see Fig. R10b], the ZPL wavelength shifts from 1064 to 1064.25 nm with increasing temperature from 20 to 65 ℃. This is consistent with our results in Fig. R13b. Moreover, the phonon wavenumber of A_{1g} mode shifts from 890.86 cm^{-1} to 890.46 cm^{-1} with increasing temperature from 296 to 338 K. As a result, the phonon-pumped lasing wavelength slightly shifts from 1175.47 to 1175.66 nm. This agrees well with our experimental results in Fig. R13c if considering measurement errors.

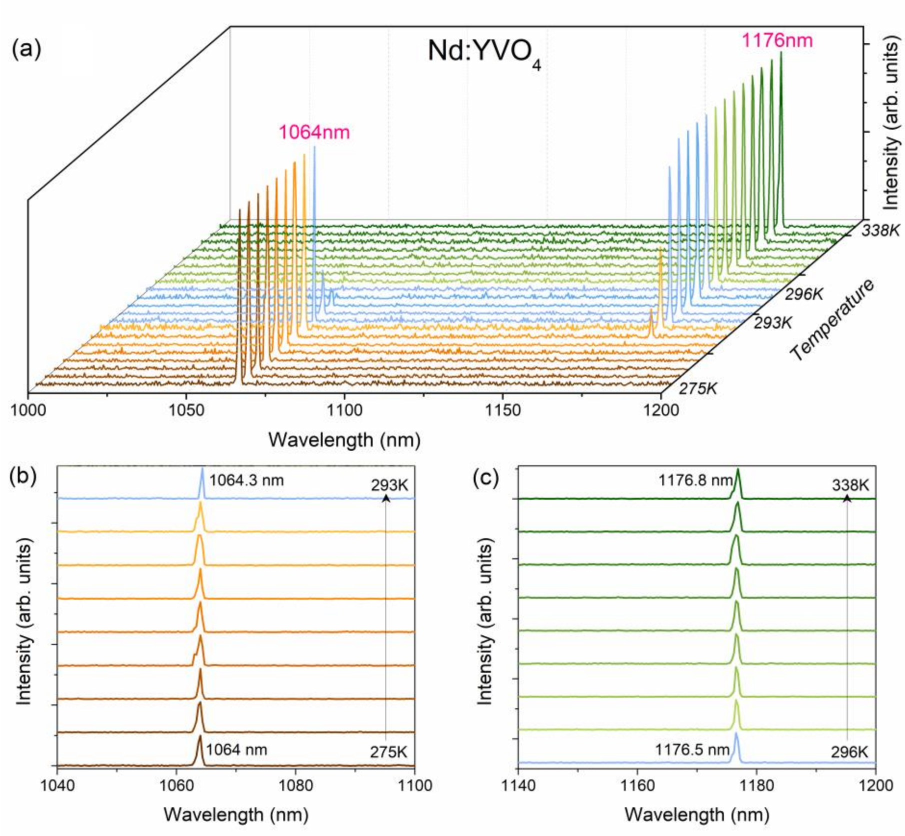

Figure R13. The phonon-pumped laser wavelengths at different temperatures.

Action:

We added these temperature dependent laser wavelengths in the Supplementary Materials (Fig. S30).

Comment:

24. Equation S13: I suggest of the authors reconsider this in a steady-state model of the laser operation.

Response:

We changed this expression. We added a new steady-state model in the revision. As stated above in *Response 12*, we gave a steady state rate equation. The population inversion maintains stabilized and the electron population densities at each level do not change with time.

Comment:

Overall, I would conclude that while the reported laser performance is impressive for an unconventional emission wavelength of Nd:YVO$_4$, and the observation of increasing oscillator strength/Huang-Rhys parameter with temperature is interesting and novel for this material, the results reported are not the transformative new type of laser that is claimed. I therefore feel that this work falls short of the level of novelty and wide readership interest that is required for publication in Nature Photonics.

Response:

As the reviewer can see, all the issues are well addressed based on the new experiments and analysis. We believe the current version does meet the strict standards on novelty, innovation, and impact for publication in ***Nature Photonics***. We sincerely hope the reviewer can change his/her recommendation.

Reviewer #3

Comment:

Summary of the key results: A laser emission in an optically pumped Nd:YAG with a wavelength selective reflection coating is observed in the vibronic regime of the fluorescence . The lasing threshold decreases when increasing the cooling temperature. From a heat conductivity model it is found that this "new" lasing occurs solely in the temperature regime above 460 K. The system thus seems to prefer heat to unlock the lasing which is counter-intuitive. They named this effect a photon-phonon collaboratively laser pumping. No insight is given into what is happening here.

Response:

Thank you for your comments. In the revision, we emphasized that our laser differs from conventional lasers. We proposed a novel phonon-pumping mechanism and an anomalous temperature dependence behavior. A critical temperature threshold was first discovered for laser generation, where the threshold-temperature (P_{th} -T_{th}) phase diagram of the present laser is ruled by $P_{th} = C/T_{th}$ (constant C upon loss), similar to Curie's Law. In addition, its lasing threshold has an anomalous temperature behavior with $\partial P_{th}/\partial T<0$, which differs from previous lasers at 1064 nm [*Ref: Journal of the Optical Society of America B, (2011), 28, 972-976*]. This is a great breakthrough innovation for laser physics and technology.

We give three important pieces of evidence to support our phonon-pumped lasing.

(1) Lasing phase diagram between 1064 and 1176 nm under different pump powers.

As shown in Fig. R14, we give two phase relation diagrams under 7.2 W pump power and 7.6 W pump power. It is clear that the phase transition temperature is dependent on the pump power. With the increasing pump power, the phase transition temperature shifts from 308 K to 293 K. This is well consistent with our phonon-pumping theory.

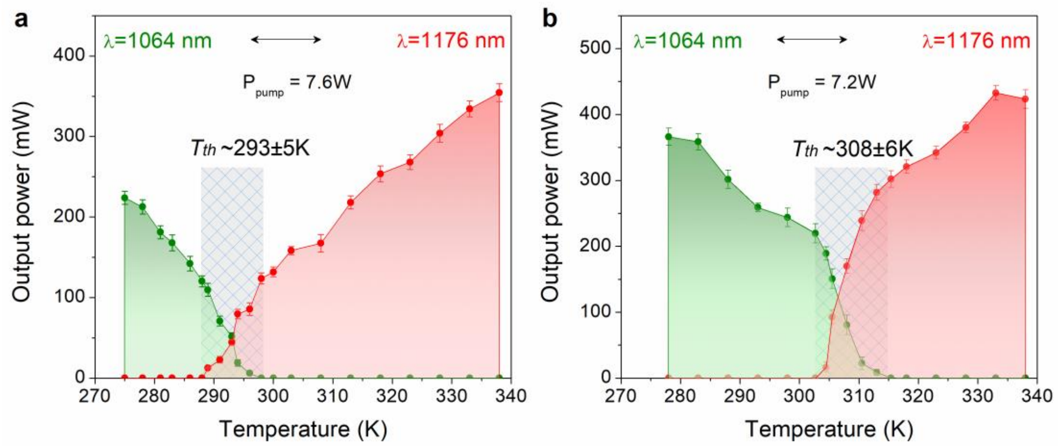

Figure R14. Power-temperature diagram of 1064 and 1176 nm laser. T_{th} is a temperature threshold for phonon-pumped lasing.

(2) We realized a tunable laser in Nd:YVO4 crystal, corresponding to various phonon modes involved in the phonon-pumping process.

In order to identify the phonon-pumping lasing, we also tried other phonon modes in Nd:YVO_4 crystal. Here, a V-shaped cavity is utilized, and a thin MgF_2 BF (d=1 mm) is inserted along Brewster's angle. By rotating the BF, we realize the lasing wavelength shift from 1176 nm to 1168 nm (Fig. R15). The participated phonon mode for 1168 nm lasing is 836 cm^{-1} (E_g mode), not 891 cm^{-1} (A_{1g} mode). This is consistent with our proposed selection rules in the main text, Fig. 3.

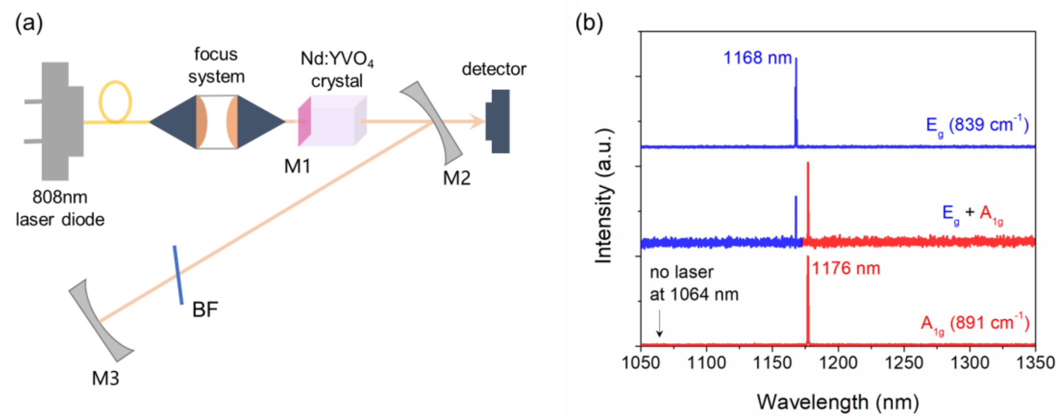

Figure R15. Tunable phonon-pumped laser in one-phonon process.

(3) **<u>We should emphasize that our used crystal is Nd:YVO$_4$ in last submission, not Nd:YAG crystal.</u>**

Our proposed phonon-pumping mechanism is also applicable in Nd:YAG crystal. In this revision, we added a similar laser result for Nd:YAG crystal in Fig. R16. Under high temperatures, Nd:YAG crystal exhibits a strengthened vibronic emission at 1151 and 1166 nm. Via a rational cavity design to suppress the conventional lasing at 946, 1064, 1122, and 1319 nm, we successfully realized a dual-wavelength lasing at 1151 and 1166 nm. These two can be well explained by the phonon-pumped laser theory. According to our calculations, the participated phonon of Nd:YAG crystal is one E_g mode at 340 cm^{-1} for 1122 nm$\xrightarrow{+340cm^{-1}}$1151 nm, and one T_{2g} mode at 719 cm^{-1} for 1064 nm$\xrightarrow{+719cm^{-1}}$1166 nm.

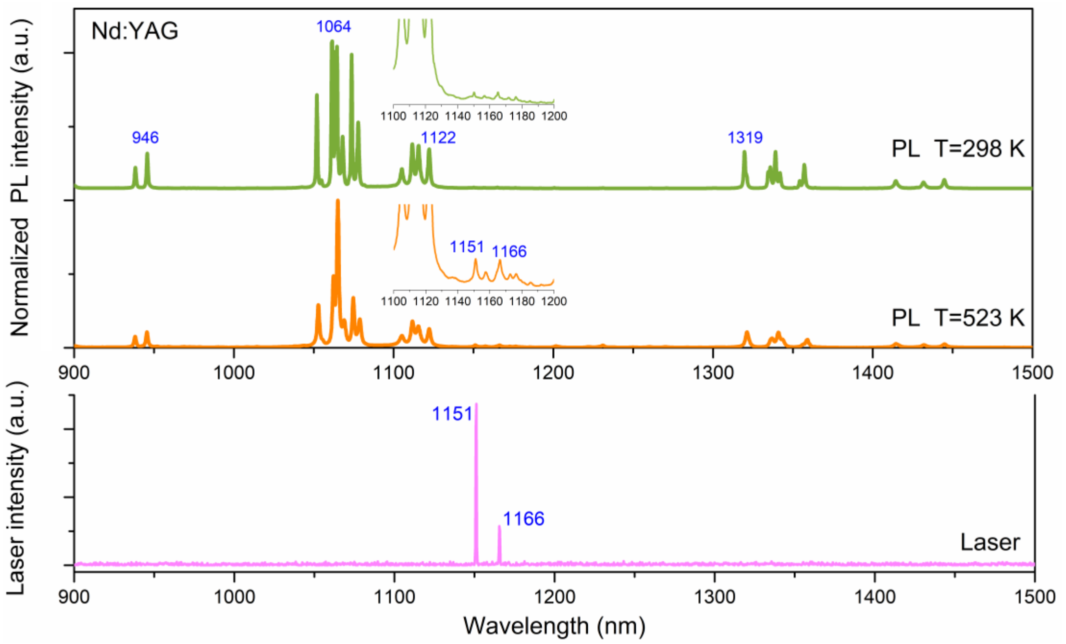

Figure R16. Fluorescence spectra (T=298 K/523 K) and phonon-pumped laser spectra of Nd:YAG crystal.

<u>Action:</u>

We have added new experimental results of Nd:YVO$_4$ crystal in the main text Fig. 4.

Comment:

Conclusions: The paper - as far as I was able to translate - does describe the experiments reasonably well. But the paper lacks a deeper understanding of the physical processes leading to the lasing. It is certainly not good enough to speculate that this effect may be caused by "a macroscopic quantum phenomena such as superconductivity"! Also, no proof is given to distinct the lasing from a Raman laser. For the relevance, the temperatures at which lasing was achieved were modest; any possible application thus merely a speculation.

Response:

First, we deleted the sentence "~~a macroscopic quantum phenomena such as superconductivity~~" in the revision. Second, we gave two evident proofs to distinct the phonon-pumped lasing from a Nd:YVO_4 Raman laser.

(1) Different lasing spectrum. As shown in Fig. R17, in self-Raman laser, it is a photon-phonon coupling process, where the high-power fundamental 1064 nm laser always exists. The output power of 1176 nm is proportional to that of 1064 nm in the resonant cavity. In our phonon-pumped laser, electron-phonon coupling is dominated and the electronic transitions of Nd^{3+} are directly modulated by the lattice vibrations. In order to obtain high-power phonon-pumped 1176 nm lasing, 1064 nm lasing must be totally suppressed. So, there is no 1064 nm lasing in our laser.

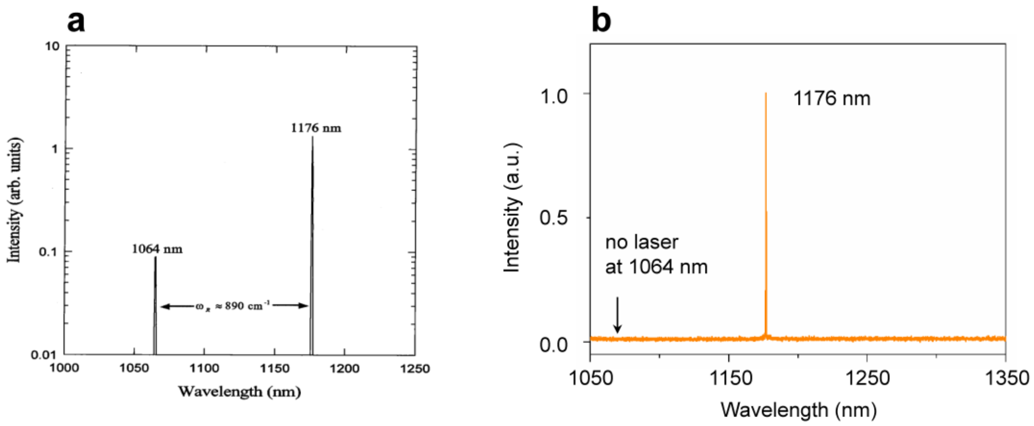

Figure R17. Laser spectrum of Nd:YVO_4 crystal, (a) self-Raman laser [Ref: *Opt. Lett.* 29, 1915-1917 (2004)], (b) phonon-pumped laser.

(2) Divergent temperature-dependent lasing performances. Raman laser doesn't have a temperature threshold, and the Raman laser intensity is directly proportional to the phonon density of states. However, our 1176 nm laser exhibited an anomalous temperature behavior that increased output power and reduced threshold at high temperatures. There is an obvious temperature threshold T_c. This differs from the previous YVO_4 Raman laser or Nd:YVO_4 self-Raman laser. In 2012, Wan. et al. reported that there was no obvious change of output power at temperatures of 5, 20, and 40 °C for 1178 nm laser in *c*-Nd:YVO_4 self-Raman laser and *c*-Nd:YVO_4/YVO_4 Raman laser [*ref: Laser Physics (2012), 22, 106-110*]. This is consistent with the result of Zverev [*ref: J. Phys. Conf. Ser. (2007), 92, 012073*], who showed that Raman gain coefficient of YVO_4 was not highly sensitive to temperature. In 2015, Ding et al. also reported a similar result in an eye-safe self-Raman Nd:YVO_4 laser at 1525 nm, that the maximum output power declined from 2.58 W to 2.38 W with increasing temperature from 10 °C to 50 °C [*ref: IEEE Photonics Journal (2015), 7, 1-7*].

Finally, we also try a wider temperature range for the phonon-pumped laser experiments. However, 65 ℃ is the highest temperature in our lab. According to numerical simulations, the central temperature of crystal is beyond 460 K. This is a sufficiently high temperature for solid-state lasers.

Action:

We have added the evident proof to distinct the lasing from a self-Raman laser in the Supplementary Materials (Fig. S32).

Comment:

Summary: Before this paper can be published, it would not only have to be improved linguistically, but also the physical models would have to be described better and deeper. Probably there is also a need for further experiments to support the statements made. Also one wishes that possible applications are not only mentioned but also justified.

Response:

Thank you for your suggestions. As you can see, we have improved the written format and rechecked our physical model with deep insights. Some conclusive evidences for phonon-pumping are present in the revision. We believe our work now is qualified for publication in *Nature Photonics*.

In addition, in the last round of submission, we wrote several possible applications, see "*Our laser platform is ready for applications in many scenarios such as high-temperature tolerant laser equipment, quantum nanophotonic, entangled phonons generation, and laser therapy with new wavelengths*". Now, we performed some additional experiments and discussions to address them.

(1) First, we provided a direct application for yellow laser generation by our phonon-pumped laser. Combining with intracavity nonlinear frequency doubling by LBO crystal, we obtained a visible yellow laser at 588 nm (Fig. R18). Similarly, this visible laser also prefers heat and exhibits improved efficiency at high temperatures. At a pump power of 10 W, the output power of yellow laser can be up to 270 mW, corresponding to a diode-to-yellow optical conversion efficiency of 2.7%. This compact yellow laser would be possible to apply in retina surgery and ophthalmology, since the oxygen-rich blood pigment, known as oxyhemoglobin, absorbs most strongly at this wavelength. [Ref] *Ophthalmic Surgery Lasers and Imaging Retina, (2012), 43(4), 341-347*

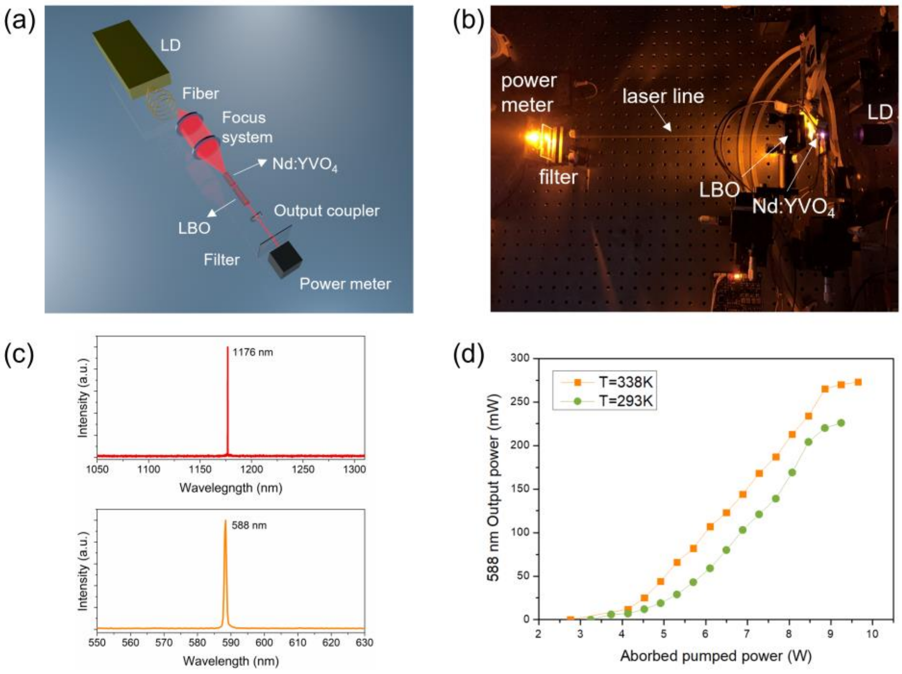

Figure R18. Yellow laser generation at 588 nm in $Nd:YVO_4$ and LBO crystal. (a) Experimental setup. (b) Yellow laser photograph. (c) Laser spectrum at 1176 and 588 nm. (d) Output powers at various temperatures.

(2) Our laser naturally supports high-temperature tolerant laser equipment because our laser performances don't deteriorate under high temperatures. Unlike with most lasers [*Refs: Laser Physics, (2018), 28(8), 085801*; *Laser Physics, (2018), 28(10), 105801*], the enhanced performance of heated Nd:YVO_4 laser devices may continue until well beyond 100 ℃ and maintain a stable lasing wavelength around 1176 nm.

(3) Our laser would also be feasible in the field of quantum nanophotonic and entangled phonons generation. Based on the selection rules, we can see that a displacive excitation of coherent phonons (DECP) would be expected when our laser is operating at 1176 nm, coupled to A_{1g} mode [*Ref: Phys. Rev. B, 1992, 45(2), 768-778*]. Moreover, when the laser is operating in ion crystals or artificial superlattices, some novel elementary excitations, such as phonon polariton and exciton polariton, can be expected. These new quasi-particles would be a promising platform for quantum nanophotonic and laser phononics. [*Refs: Phys. Rev. Lett. (2010), 105, 196402; Nature (2020), 583, 780-784*]

More importantly, our work would open new research spots for four-level laser systems, from which their temperature behaviors have been neglected for a long time. This phonon-pumping mechanism can be feasible in many laser materials and bring great opportunities for wavelength extension and power improvement. Meanwhile, this phonon-pumping effect is also a breakthrough for conventional laser physics. The vibronic effect is equally important in those weak electron-phonon-coupling systems.

Action:

We have added the experimental results of yellow laser in the revision. We added some discussions in Page 14.

As you can see, we have successfully addressed all the issues. Thanks to the his/her comments, our manuscript's quality has significantly improved. We believe our work now is qualified for publication in *Nature Photonics*.

A list of changes:

Text

We slightly revised the abstract and introduction parts.

Several sentences have been added to address the reviewers' comments, especially for lasing mechanism, and temperature-dependent laser wavelengths.

Figures

According to reviewer's suggestion, we corrected Fig. 1, Fig 2, and Fig. 4 in the main text.

References

Ref 22, 23 have been deleted in the main text.

Supplementary information

Additional extended Fig. S1, S8-S10, S14-S18, S20-S26, S30, Table S1-S2, and explanatory text have been added in the supplementary materials.